Multi-target tracking pipeline for MIMO-FMCW radars based on modified GM-PHD

S. Hamed Javadi[1], Ruoyu Feng[1], André Bourdoux[1], Hichem Sahli[1,2]
[1]*IMEC, Kapeldreef 75, B-3001 Leuven, Belgium*
[2]*Informatics Dept., Vrije Universiteit Brussel (VUB), Pleinlaan 2, 1050 Brussels, Belgium*

***Abstract*—Multitarget tracking (MTT) with radar is challenging due to the radar's low-resolution noisy clutter-prone observation data. Classical approaches employ data association filters to deal with clutter and interference, but they are highly complex. This paper presents an improved Gaussian mixture probability hypothesis density (GM-PHD) multi-target tracking pipeline. The proposed GM-PHD solution considers (i) radar bounding-box-based measurements, (ii) a clutter model for radar observations, and (iii) robust target identification. Using both simulated and experimental scenarios, these contributions are proven to improve the tracking performance in terms of robustness against noise and clutter, as well as target identification. The significance of the presented MTT scheme lies in its low complexity since it does not need any data association. This makes it applicable for intense high-level applications for which MTT is used.**

***Index Terms*—Frequency modulated continuous wave (FMCW); Gaussian mixture (GM); multiple-input-multiple-output (MIMO); multi-target tracking (MTT); probability hypothesis density (PHD) filter; radar.**

I. Introduction

RADARS were initially used for target detection and ranging [1]. They provide information on the existence of targets in different ranges and angles with limited resolution. The information can then be used for instantaneous tracking of targets via an appropriate multitarget tracking (MTT) algorithm [2]. Classical approaches tackle MTT by applying a single target Kalman Filter (KF) — or one of its extensions such as extended KF (EKF) or unscented KF (UKF) — on each detected state along with an appropriate data association filter. Moreover, they do pruning of less likely states and merge close states to avoid exploding the number of states. Popular MTT algorithms are multiple hypotheses tracking (MHT) [3] and joint probabilistic data association filter (JPDAF) [4].

JPDAF computes the joint probabilities of correct association and uses them to update each track. Alternatively, MHT establishes a hypothetical track per valid measurement and treats each track independently. In JPDAF and MHT, a multitarget state is represented by vectors which pose limitations for calculating the estimation error, mainly when the estimated number of states differs from the actual one. To alleviate this drawback, Mahler in [5] adopted finite set statistics (FISST) for MTT and derived the Bayesian filter recursion based on the probability hypothesis density (PHD) function that propagates the posterior intensity function.

The research leading to these results has received funding from IMEC.ICON and Flanders Innovation & Entrepreneurship (nr HBC.2020.3106) – Project Surv-AI-llance.

Approximating the intensity function as a mixture of Gaussian components makes the PHD recursion tractable and gives rise to the Gaussian mixture (GM) PHD filter [6], [7]. The PHD filters, including GM-PHD, essentially do not need any data association filter[1]. Hence, they are computationally lighter than the classical MTT approaches [2], [9].

During recent decades, the advances in small-size multiple-input-multiple-output (MIMO) radars in mm-wave frequencies have significantly improved the radar resolution and made them an indispensable robust sensing unit in civilian applications such as automotive industry [10] and smart homes [11]. However, a higher radar resolution gives multiple range-Doppler (or range-azimuth) bins per target, giving rise to so-called *extended targets*. At the same time, the MTT algorithms are used to assume one measurement per target. While algorithms exist for extended target tracking [12], they are complex. They may not be appropriate for edge applications (e.g., automotive) where tracking is only a part, and the complexity should be avoided due to the edge resource limitations. A less complex alternate is to cluster targets and represent each target by the centroid of its cluster [11].

In this paper, we improve the GM-PHD filter for radar multi-target tracking. The contributions presented in this paper are as follows:

- To the extent of the authors' knowledge, this is the first published PHD-based MTT pipeline, including the whole signal processing chain for a MIMO-FMCW radar;
- We propose a clutter model based on the *radar* observation data. This clutter model results in better calculations of the weights of the Gaussian components and brings more robustness;
- We propose to modify the radar measurements, namely, the range and velocity, based on the bounding boxes indicating the point cloud intervals of each target. To this end, we generate an association matrix based on the likelihood of each measurement given the predicted measurements and select the most appropriate cluster point instead of its centroid;
- The effectiveness of the proposed radar MTT pipeline is shown through both simulated and experimental scenarios using a MIMO-FMCW radar to track pedestrians.

[1]Though data association is used in some works to improve tracking track identities (e.g., [8]), it is optional.

II. Background

A. FMCW radar basics

A Frequency-Modulated Continuous-Wave (FMCW) radar uses a continuous wave (CW) signal that is frequency-modulated over a certain bandwidth B:

$$s_{chirp}(t) = a_c \exp\left[j2\pi\left(f_c + \frac{\alpha}{2}t\right)t\right]\Pi\left(t/T_c\right), \quad (1)$$

where a_c and T_c respectively denote the amplitude and the period of the transmitted chirp, $\alpha = B/T_c$ is its frequency slope, and $\Pi\left(t/T_c\right)$ equals 1 for $0 < t < T_c$ and 0 elsewhere. A target then reflects the transmitted signal, and the received signal is mixed with the original transmitted signal to generate the beat signal, whose frequency is shifted due to the target's range and range rate. In sufficiently high bandwidths, the beat signal becomes separable in fast time (indicating intra-chirp samples) and slow time (indicating inter-chirp samples). This allows applying a 2D Fourier transform (FT) along the fast and slow times to obtain the range-Doppler (RD) map corresponding to the target(s).

In multiple-input-multiple-output (MIMO) radars, an RD-map is obtained per virtual antenna. Hence, a data cube, instead of a matrix, is available. Here, beamforming is performed by applying a third FT along the third dimension to get the azimuth information.

B. GM-PHD filter

In GM-PHD, each state is expressed as a Gaussian component with a specific tag used for identification. The Gaussian component with a unique tag t_j at instant k is represented by $\nu_k^{(t_j)}(x) \triangleq w_k^{(t_j)}\mathcal{N}\left(x; m_k^{(t_j)}, P_k^{(t_j)}\right)$ where $m_k^{(t_j)}$ and $P_k^{(t_j)}$ denote the mean and the covariance matrix of the Gaussian component, respectively, and $w_k^{(t_j)}$ is its weight. The reader can find the detailed original recursion equations in [6]. A summary of the slightly modified GM-PHD filter implemented in the current work follows.

Let's assume the linear process equation and a general observation model for each Gaussian component:

$$\begin{aligned} f_{k|k-1}(x|x_{k-1}) &= \mathcal{N}\left(x; Fx_{k-1}, Q\right), \\ g_k(z|x_k) &= \mathcal{N}\left(z; h\left(x_k\right), R\right), \end{aligned} \quad (2)$$

where F is the process matrix of the constant velocity model with process noise covariance Q, and $h(.)$ is a generic measurement model with R being its corresponding noise covariance matrix. Then, the GM-PHD recursion involves the iteration of the following steps [6].

1) Prediction: Given the states in the last instant, the predicted PHD function is given by:

$$\nu_{k|k-1}(x) = \sum_{j=1}^{J_{k-1}} p_s \nu_k^{(t_j)}(x) + \nu_{\beta,k|k-1} + \nu_{\gamma,k}(x), \quad (3)$$

where p_s is the survival probability (a design parameter), J_{k-1} denotes the number of the states (i.e., Gaussian components) in the last instant, and $\nu_{\beta,k|k-1}$ and $\nu_{\gamma,k}$ are respectively the spawned and instantaneous birth PHDs given respectively by:

$$\begin{aligned} \nu_{\beta,k|k-1} = \sum_{j=1}^{j=J_{k-1}} \sum_{i=1}^{J_{\beta,j}} w_s w_{k-1}^{(t_j)} \mathcal{N}(x; Fm_{k-1}^{(t_j)} + d_i, \\ FP_{k-1}^{(t_j)}F^T + Q_\beta), \end{aligned} \quad (4)$$

and $\nu_{\gamma,k}(x) = \sum_{j=1}^{J_{\gamma,k}} \nu_{\gamma,k}^{(t_j)}(x)$. In these equations, $J_{\beta,j}$ is a Poisson random variable (r.v.) with a specified rate and denotes the number of spawned states from state t_j, and w_s, d_i, and Q_β are given design parameters. Similarly, $J_{\gamma,k}$ is a Poisson r.v. denoting the number of born states at instant k. $\nu_{\gamma,k}^{(t_j)}(x)$ denotes the PHD of the jth born state with a random mean and a large covariance (e.g., we used $P_{\gamma,k}^{(t_j)} = 40P_0$ where P_0 is the initial covariance.). The spawned states are assigned unique tags.

2) Measurements modification and gating: The measurements are detected with probability p_d (a design parameter). The measurements are modified as elaborated in Sec. III-A. Then, the modified measurements whose normalized innovation squared do not fall within the gates of the predicted measurements are removed.

3) Update: The detected and modified measurements contribute to updating the set of states as follows:

$$\nu_k(x) = (1 - p_d)\,\nu_{k|k-1}(x) + \sum_{i=1}^{J_{Z_k}} \sum_{j=1}^{J_{k|k-1}} \nu_{k|k}^{(t_j)}(x_{k|k-1}, z_i), \quad (5)$$

where Z_k is the set of the detected measurements with cardinality $J_{(Z_k)}$. The mean and the covariance of each component $\nu_{k|k}^{(t_j)}$ are calculated using the extended Kalman filter (EKF) recursion. The weight is updated by:

$$w_{k|k}^{(t_j)} = \frac{p_d w_{k|k-1}^{(t_j)} q_k^{(t_j)}(z)}{\kappa_k(z) + p_d \sum_{l=1}^{J_{k|k-1}} w_{k|k-1}^{(t_j)} q_k^{(t_l)}(z)}, \quad (6)$$

in which $q_k^{(t_j)}(z)$ is the association probability of measurement z to the predicted measurement of state t_j:

$$q_k^{(t_j)}(z) = \mathcal{N}\left(z; h\left(x_{k|k-1}^{(t_j)}\right), R + H_k P_{k|k-1}^{(t_j)} H_k^T\right), \quad (7)$$

wherein H_k is the Jacobian matrix and $P_{k|k-1}^{(t_j)}$ denotes the predicted estimation error covariance matrix of state t_j. At the end of this step, the tags are not unique anymore. This will be corrected after pruning and merging. Also, $\kappa_k(z)$ denotes the clutter intensity, which is key in determining the weights' values. The clutter modeling is discussed in Sec. III-B.

4) Pruning and merging: To avoid the exponentially growing number of the Gaussian components, the components with weights less than a threshold (a design parameter) are omitted, and the other weights are modified to maintain the exact summation as before pruning. Afterward, close components are merged to create a single component. Merging is carried out iteratively. At each step, the component with the most stable tag (i.e., the tag that has existed more during previous

recent instances) is selected, and the components in its vicinity are merged. The other merging steps are the same as elaborated in [7].

5) States selection: Finally, among the Gaussian components, those with a weight more than a threshold (say, 0.5) are selected as the set of the current states. In contrast, others still contribute to updating the states in later instances.

III. FMCW RADAR MTT PIPELINE

Fig. 1 depicts the MTT pipeline with the radar data cube as input. First, the static targets are removed by subtracting the average of all chirps from all those chirps. This is done per antenna. Then, the 3D Fourier Transform (3D-FT) gives the range, velocity, and azimuth of the potential existing moving scatterers, which are detected using an appropriate Constant False Alarm Rate (CFAR) detector (e.g., the smallest of cell averaging (SOCA) CFAR [13]). The detected range-Doppler bins are then clustered using DBSCAN [14]. DBSCAN gives two outputs: i. the centroids of the clusters ($[c_k]$ in Fig. 1) are fed into MUSIC [13] to fine-tune the azimuth calculation[2]; and ii. the bounding boxes of the clusters used in measurement modification are explained below.

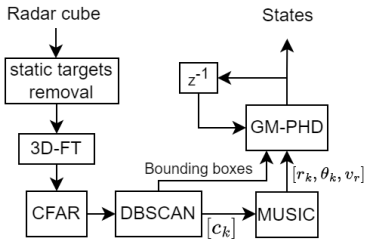

Fig. 1. An overview of the radar MTT pipeline.

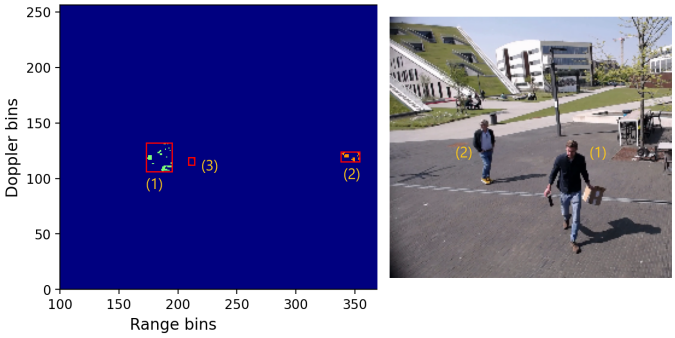

Fig. 2. An example of clustering of the target's point clouds in the RD map. Clusters (1) and (2) belong to the corresponding targets shown in the camera image, while (3) indicates clutter, probably due to multi-path.

[2]This is optional. Instead, the range, Doppler, and azimuth corresponding to the bins given by DBSCAN can be directly used as inputs by GM-PHD. However, the angular resolution of the radar is coarse, and a super-resolution algorithm is needed for fine-tuning.

A. Radar measurements

The detected bins are clustered using DBSCAN (see Fig. 2). It is common to consider the centroid of each cluster as the representative of the radar measurement. However, this may not be the optimal representation. Alternatively, we propose using the closest point of the cluster in terms of its likelihood, given the predicted measurements.

To choose the best cluster representation, an association matrix $A_k = [a_{i,j}]$ is created with $a_{i,j} \triangleq q_k^{(t_j)}(z_{ij}^\star)$ where $z_{ij}^\star$ is the closest point of the cluster of z_i to the predicted measurement of state t_j. Each measurement z_i is replaced with the point that gives the highest likelihood in row i of A_k. Specifically, $z_i \leftarrow \arg\max\, q_k^{(t_j)}(z_{ij}^\star)$.

As an example, Fig. 3 shows four bounding boxes. Since there are two predicted measurements ($\hat{z}_1$ and $\hat{z}_2$), there are at most two closest points per bounding box (marked by red X), each corresponding to a predicted measurement. The association probabilities of these closest measurements (i.e., red Xs) to the predicted measurements (gray stars) are calculated, and the one with the highest association probability is used as the cluster representative (indicated by small green stars in Fig. 3).

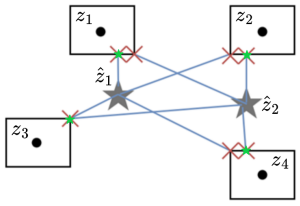

Fig. 3. Modification of the measurements based on their bounding boxes.

This modification increases the likelihood of the measurements (Eq. (7)) and results in more stable weights (Eq. (6)). Hence, it effectively impacts the PHD filter performance.

B. Clutter modeling

Clutter is the other determining value in Eq. (6). A common approach is to model the clutter as uniformly distributed measurements, i.e., $\kappa(z) = \lambda u(z)$. This model does not fit in the radar MTT pipeline. Indeed, there are three clutter sources in a radar's RD map: i. speckle noise; and ii. multi-path clutter (e.g., see Fig. 2); and iii. clutter due to wrong clustering. The first clutter type is effectively suppressed by DBSCAN. The other two clutter types depend on the states. Accordingly, we model the clutter intensity as:

$$\kappa_k(z) = \lambda_c \frac{1}{a} \sum_{j=1}^{J_{k|k-1}} w_{k|k-1}^{(t_j)}\,, \tag{8}$$

where a denotes the area of the radar's field of view (FoV)[3] and λ_c is the clutter rate given as a Poisson r.v. with a specified average rate $\bar{\lambda}_c$ (e.g., we used $\bar{\lambda}_c = 2$ based on our

[3]If the radar has a 180^o FoV, $a = \frac{\pi}{2} R_{max}^2$ with R_{max} being the maximum radar unambiguous range.

observation). Note that the clutter model (8) does not explicitly depend on the measurement z but it implicitly depends on the measurements in the previous step through $w_{k|k-1}^{(t_j)}$.

C. Robust target identification

The original GM-PHD filter uses the strongest component (i.e., the component with the largest weight) for merging [7]. However, this is a hard selection since the weights are not too far from each other and may result in emerging new target tags. To have a more robust target identification, as discussed in step 4 of Sec. II-B, we use the most stable tag at each iteration of merging.

IV. Evaluation Results

A. Simulated evaluation

We evaluate the implemented modified GM-PHD filter using a simulated scenario for tracking 8 targets moving in different velocities and directions as shown in Fig. 4-a where each color indicates a specific target. The radar in $[0, 0]$ measures range, azimuth, and Doppler and uses a white noise acceleration model. The scenario includes two targets (blue and black) moving toward each other; two targets (green and red) moving from left to right and crossing each other; two targets (green and cyan) moving from left to right, joining each other, and then splitting; two targets (gray and violet) moving from left to right, the gray first starts moving, then the violet appears and reaches the gray, then the gray stops while the violet goes up. All target motions consist of stages of accelerating, constant velocity and slowing down. The trajectories of the targets are contaminated by a Gaussian noise to simulate the uncertainty of the measurements caused by vibrations, non-rigid targets, clustering, and observation noise. The range and Doppler variances are both 0.1 while the azimuth variance is 0.01. Furthermore, a Poisson-distributed random number of clutters per target with an average rate of 2 are added.

The GM-PHD parameters are listed in Table I. Fig. 4-b depicts the tracking result given by the proposed GM-PHD algorithm where the color change indicates the change in the target identification (i.e., its tag). Fig. 4-c and d compare the performance of the algorithm with JPDAF in terms of the Hausdorff distance and the number of the detected targets. The implemented JPDAF uses the same single target parameters and EKF as GM-PHD. The comparison shows the superiority of GM-PHD over JPDAF. Note that GM-PHD does not perform data association and, hence, is computationally lighter than JPDAF.

TABLE I
The setting of GM-PHD in evaluation.

	Prune Thresh.	Merge Thresh.	p_d	p_s	$\bar{\lambda}_c$	Max. no. of components
Value	10^{-5}	4	0.99	0.99	2	200

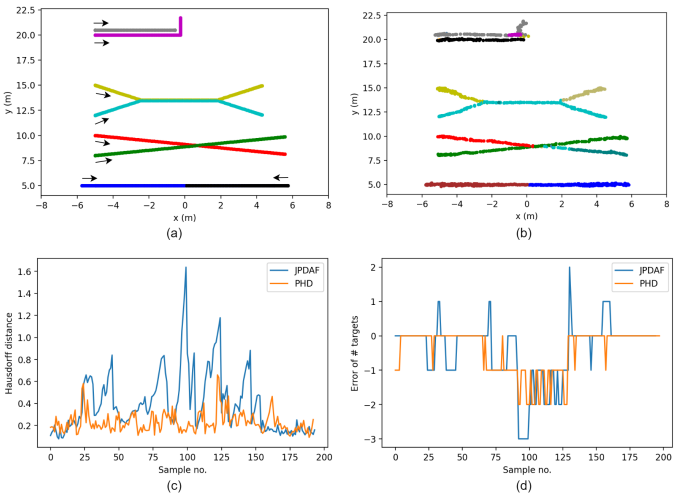

Fig. 4. Evaluation of our PHD-based MTT algorithm in a simulated scenario. (a) Ground truth. (b) The PHD-based tracking result. (c) and (d) compare the PHD- and JPDA-based algorithms in terms of the Hausdorff distance and the error in estimating the number of targets, respectively.

B. Experimental evaluation

We evaluate the performance of the whole radar-based MTT pipeline (Fig. 1) in the tracking of pedestrians in a semi-public environment. The setup included a TI IWR6843ISK of Texas Instruments which is a MIMO FMCW radar with three transmitters and four receivers. It was installed together with a commercial webcam (HD Pro of LogiTech) on a tripod at a height of around $3m$ from the ground and a tilt of around 13^o towards the ground. The radar setting is listed in Table II. The setting of the GM-PHD filter is also the same as Table I.

TABLE II
The setting of the radar used for experimental evaluation.

Radar parameter	Value
Start frequency (GHz)	60.1221
Bandwidth (GHz)	3.257
Pulse repetition time (μs)	36.66
Coherent processing time (ms)	90
Number of chirps per frame	255
Number of samples per chirp	256
Sampling frequency (MHz)	9.6

Fig. 5 illustrates an image of the area of data recording as well as an example of the estimated tracks during one minute in two cases with and without measurement modification using the bounding boxes. As seen, the clutter removal and target identification are more robust when the radar measurements are modified using bounding boxes.

Furthermore, the consistency of the GM-PHD was analyzed in terms of the total normalized innovation squared (NIS) in the two cases (with and without measurement modification). For consistency analysis, the GM-PHD was run 10 times and the NIS values of the calculated states are averaged. The consistency analysis results are shown in Fig. 6 in the two cases together with the 95% confidence limits as well as

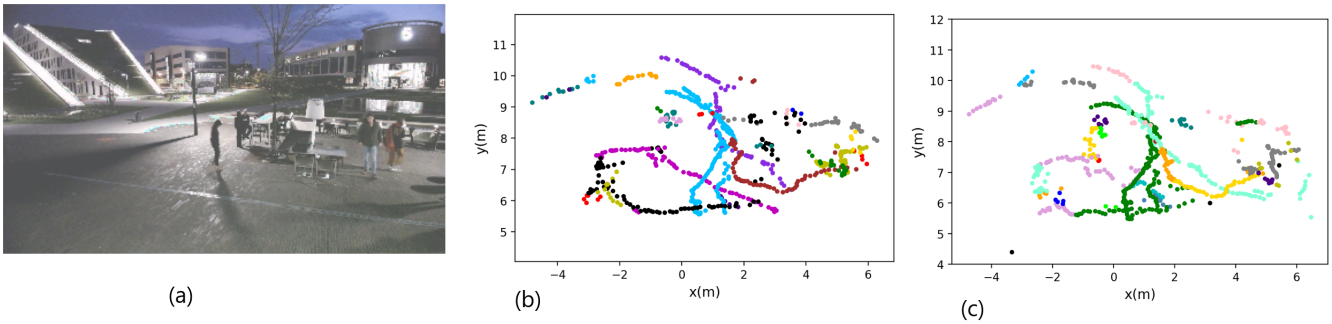

Fig. 5. Evaluation of the PHD-based MTT with real radar data. (a) The scene of radar recording. (b) Tracking routes when bounding-box-based measurements are used. (c) Tracking routes without bounding boxes. In (a) and (b), color changes indicate different target IDs.

their moving average. As seen, measurement modification also brings more consistency to multitarget tracking.

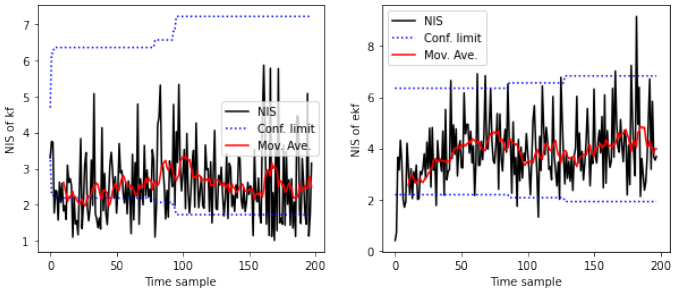

Fig. 6. Normalized innovation squared (NIS) in two cases of (a) with bounding-box-based measurements; and (b) without bounding boxes.

V. Conclusion and Future Directions

In this paper, we presented a radar MTT pipeline based on a modified GM-PHD filter. The pipeline includes the necessary steps for processing a MIMO-FMCW radar, namely statistical target removal, 3D-FT, and CFAR detection. Then, DBSCAN is used to cluster the extended targets given by detection. Then, the centroids of the clusters are used as the raw measurements by GM-PHD while their corresponding bounding boxes are used for fine-tuning the measurements based on the predicted measurements from the previous instant. Furthermore, we introduced a more fitting clutter model for processed radar data to be used in GM-PHD formulations. In the end, we demonstrated the robustness of the proposed modifications through experimental tracking of pedestrians using a 60GHz MIMO radar.

The tracking results highly depend on the quality of its input data. As a future study, the impact of other kinds of CFAR detectors, such as GLRT-CFAR, on the tracking performance can be studied. Furthermore, the GM-PHD filter can be replaced with its cardinalized version (i.e., GM-CPHD). Note that both improvements would significantly increase the MTT complexity.

Acknowledgment

The research leading to these results has received funding from IMEC.ICON and Flanders Innovation & Entrepreneurship (nr HBC.2020.3106) – Project Surv-AI-llance.

References

[1] S. H. Javadi, "Detection over sensor networks: a tutorial," *IEEE Aerosp. Elect. Syst. Mag.*, vol. 31, no. 3, pp. 2–18, 2016.

[2] S. H. Javadi and A. Farina, "Radar networks: A review of features and challenges," *Inf. Fusion*, vol. 61, pp. 48–55, 2020.

[3] D. Reid, "An algorithm for tracking multiple targets," *IEEE Transactions on Automatic Control*, vol. 24, no. 6, pp. 843–854, 1979.

[4] Y. Bar-Shalom and X. Li, *Multitarget-Multisensor Tracking: Principles and Techniques*. Storrs, CT: YBS Publishing, 1995.

[5] R. Mahler, "Multitarget Bayes filtering via first-order multitarget moments," *IEEE Transactions on Aerospace and Electronic Systems*, vol. 39, no. 4, pp. 1152–1178, 2003.

[6] B.-N. Vo and W.-K. Ma, "The Gaussian Mixture Probability Hypothesis Density Filter," *IEEE Transactions on Signal Processing*, vol. 54, no. 11, pp. 4091–4104, 2006.

[7] D. E. Clark, K. Panta, and B.-n. Vo, "The gm-phd filter multiple target tracker," in *2006 9th International Conference on Information Fusion*, 2006, pp. 1–8.

[8] K. Panta, D. E. Clark, and B.-N. Vo, "Data association and track management for the gaussian mixture probability hypothesis density filter," *IEEE Transactions on Aerospace and Electronic Systems*, vol. 45, no. 3, pp. 1003–1016, 2009.

[9] B.-T. Vo, B.-N. Vo, and A. Cantoni, "Analytic implementations of the cardinalized probability hypothesis density filter," *IEEE Transactions on Signal Processing*, vol. 55, no. 7, pp. 3553–3567, 2007.

[10] A. Venon, Y. Dupuis, P. Vasseur, and P. Merriaux, "Millimeter Wave FMCW RADARs for Perception, Recognition and Localization in Automotive Applications: A Survey," *IEEE Transactions on Intelligent Vehicles*, vol. 7, no. 3, pp. 533–555, 2022.

[11] A. Gorji, H.-U.-R. Khalid, A. Bourdoux, and H. Sahli, "On the generalization and reliability of single radar-based human activity recognition," *IEEE Access*, vol. 9, pp. 85 334–85 349, 2021.

[12] G. Gennarelli, G. Vivone, P. Braca, F. Soldovieri, and M. G. Amin, "Multiple extended target tracking for through-wall radars," *IEEE Transactions on Geoscience and Remote Sensing*, vol. 53, no. 12, pp. 6482–6494, 2015.

[13] M. A. Richards, *Fundamentals of Radar Signal Processing*. NY, USA: McGraw-Hill Education, 2014.

[14] M. Ester, H.-P. Kriegel, J. Sander, and X. Xu, "A density-based algorithm for discovering clusters in large spatial databases with noise," in *Proceedings of the Second International Conference on Knowledge Discovery and Data Mining*, ser. KDD'96. AAAI Press, 1996, p. 226–231.